Geologie en Mijnbouw **71**: 337–349, 1993.

Biotite crystallization temperatures and redox states in granitic rocks as indicator for tectonic setting

Dorothee J.M. Burkhard
Institute of Earth Sciences and Debye Institute, University of Utrecht, 3508 TA Utrecht, The Netherlands

Received 20 August 1992; accepted in revised form 19 January 1993

Key words: Australia, Japan, Alps, Portugal, oxygen fugacity

Abstract

A T-fO$_2$ pair is the result of solving two independent equations (for biotite and its host rock) each of which relates the two unknowns, oxygen fugacity (fO$_2$) and temperature, with an analytically determined Fe^{2+}/Fe^{3+} ratio. T-fO$_2$ pairs, determined for a series of rock samples from localities which are spatially distributed over an intrusive are different and plot linearly in 1/T-log$f$O$_2$ space. A comparison of such lines, estimated for granites from Australia, Japan and Portugal shows three major features: (1) magnetite-granites and magnetite-free ilmenite-granites cover distinct fields, (2) Australian granites have a lower oxidation state and higher biotite crystallization temperatures than granites from Japan, and (3) ilmenite-granites from Japan plot systematically in an oxygen-rich regime, that is above the NiNiO (NNO) buffer, implying that their mineral assemblage is not in equilibrium whereas ilmenite-granites from Australia plot in an oxygen-poor regime, i.e. below the fayalite-magnetite-quartz (FMQ) buffer.

It is, of course, expected that magnetite-free ilmenite-granites with all Fe^{3+} partitioned into biotite, have an oxidation state below (FMQ). Ilmenite-granites which plot above (FMQ) must therefore have experienced oxidation upon cooling, after ilmenite and after biotite crystallization. Such an oxidation may be related to volatile water, available at temperatures below water saturation and above solidification of the rock. Because ilmenite-granites plot either below or above (FMQ) for a specific region, one may infer that this is related to a regionally low or high water content respectively. As such one can distinguish low-water regions, such as Australia and N Portugal which are recognized as non-subduction-related granites, and high-water regions, such as Japan and the Alps (Bergell) which are recognized as subduction-related granites. It is concluded that in non-subduction-related regimes the redox state of the source rock has been preserved in contrast to rocks in subduction-related regimes.

Introduction

The oxygen fugacity (fO$_2$) is a temperature-dependent intensive parameter which controls the oxidation state and therefore the partitioning of multivalent transition elements between a melt and its crystallizing minerals. Because of the temperature dependence, only an estimate can usually be made of the redox state of a mineral. In granite petrology, interest in fO$_2$ has arisen mainly from a possible causal relation between the redox state of a granite and the occurrence of ore deposits (Ishihara 1977, 1981). Due to the fact that granites contain quartz, the presence or absence of magnetite (Fe^{2+}Fe$_2^{3+}$O$_4$) allows rough estimates of the redox state with respect to the fayalite-magnetite-quartz (FMQ) buffer. Determination of the redox trend, which requires knowledge of T-fO_2 pairs, might be achieved by analyzing two different Fe-bearing minerals in equilibrium, both with a specific sensitivity to fO_2 and temperature. In granites, there are only a few Fe-bearing minerals among which Fe-Ti oxides and biotite. The ease with which, in particular ulvöspinel, looses Ti and adjusts its chemistry to low-temperature events of late-magmatic alteration, makes it unsuitable to trace magmatic conditions by means of Fe-Ti oxide geobarometers (method of Buddington & Lindsley 1964), hence leaving biotite as the only appropriate candidate.

In view of the above I have suggested a method to estimate T-fO_2 pairs of biotite-bearing intrusions (Burkhard 1991) based on the analytically determined Fe^{2+}/Fe^{3+} ratio of biotite and the bulk rock. For both, biotite and rock, fO_2 can be inferred as a function of temperature, based on this ratio (Hewitt 1981 in Wones 1981, Kress & Carmichael 1988).[1] In spite of the fact that my method requires an extrapolation of physico-chemical parameters from high-temperature data (ca. 1300° C) to temperatures of granite crystallization (ca. 800° C), it shows promise. The calculated temperatures and fO_2 values for sample sets of two different granites gave the following results: (1) redox states of magnetite-granites and magnetite-free ilmenite-granites (ilmenite, $Fe^{2+}TiO_3$) occur above respectively below (FMQ) in accordance with presence or absence of magnetite; (2) calculated varying temperatures, as well as T and fO_2 ranges, could be interpreted as being due to variations of water available during granite emplacement; (3) after a critical evaluation of the effect of late- or post-magmatic alteration I could infer that T-fO_2 pairs of a particular intrusive, which plot linearly in 1/T-logfO_2 space, delineate the evolution of fO_2 as a function of temperature.

This encouraging result gives confidence in the usefulness of the method, and urges a comparison of these parameters between different granites. Such a comparison is presented here between granites from the Lachlan Fold Belt, Australia, and granites from Japan and N Portugal. I find that in a non-subduction-related tectonic setting, fO_2 reflects the redox state of the source rock in magma systems with relatively low water content, whereas in subduction-related settings the original redox state becomes obscured in a high-water environment during emplacement. Ilmenite-granites are sensitive to whether a granite emplacement occurred under low or high-water conditions.

Method

Samples with fresh biotite, no chlorite or muscovite alteration, and a minimum of opaque inclusions in the biotite were selected for T-fO_2 studies from a comprehensive collection of Australian granites (see Appendix).

The calculation of T-fO_2 pairs (Burkhard 1991) is based on the assumption that fO_2, defined by the redox state of the melt, determines the partitioning of Fe^{3+} and Fe^{2+} between crystallizing biotite and melt, and that biotite crystallizes in its stability field with respect to composition, T and fO_2. Temperature and fO_2 value are the two unknowns which are calculated from two equilibrium equations for the T dependence of fO_2 for biotite (Hewitt 1981 in Wones 1981), and for the bulk rock (e.g. Kress & Carmichael 1988). The calculation of T-fO_2 pairs of a sample requires (1) the bulk composition in terms of major element oxides in order to calculate the melt parameters such as Margules terms, (2) knowledge on presence of magnetite to assess its activity, and (3) electron microprobe analyses on biotite, feldspar and amphibole, to determine the total Fe content of biotite and the activity of sanidine, and to estimate total pressure by means of a hornblende geobarometer (e.g. Hollister et al. 1987). Fe^{2+} has to be analyzed (the accuracy of wet chemical analyses suffices) for bulk rock and biotite to determine their ferrous and ferric iron content.

Further details on the calculation are given in Burkhard (1991) and in the Appendix. The calculated temperatures and fO_2 values and data on the

---

[1] It has been argued that these equations do not take into account oxidizing agents like F or CO_2 and hence are not valid. However, it is the combined effect of oxidizing and reducing agents which characterizes the redox state of the system and determines the Fe^{3+}/Fe^{2+} ratio.

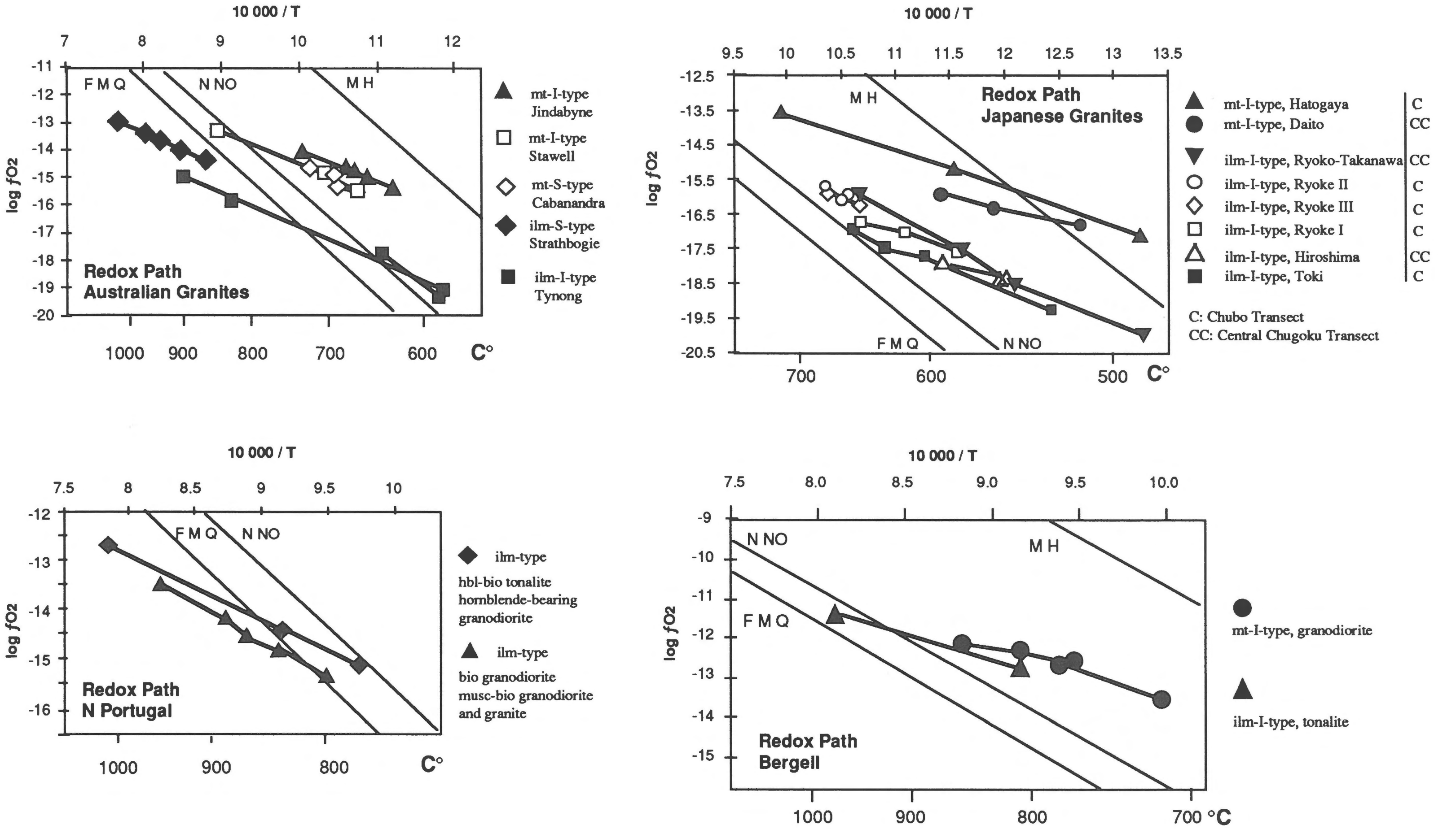

Fig. 1. T and log fO_2 values of granites from Australia, N Portugal, Japan and the Swiss-Italian Alps (Bergell intrusives, Burkhard, unpubl.). Values from N Portugal are calculated from data given by De Albuquerque (1971, 1973). For Australia and N Portugal, magnetite-free (ilmenite-) granites tend to plot below the FMQ buffer as expected for a rock without magnetite. Ilmenite-granites from Japan and the Alps tend to plot above the FMQ buffer. This indicates a disequilibrium because these rocks do not bear magnetite. Inflections in the redox paths are related to multi-intrusive bodies, and are in contrast to smooth lines for Australia where each point represents a single intrusion. Buffers are taken from Huebner (1971).

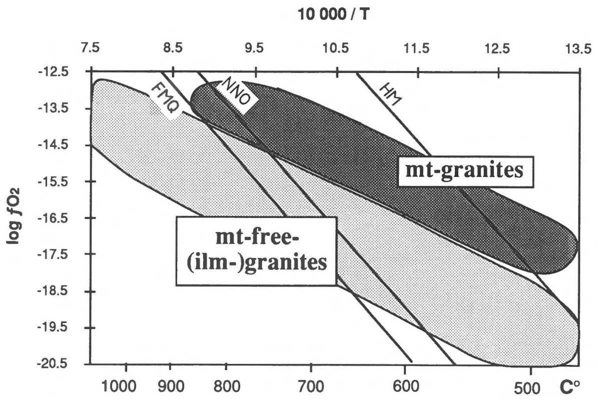

Fig. 2. Redox path of the Australian and Japanese granites. Fields of magnetite and magnitite-free ilmenite-granites are quite distinct, and all granites follow a similar redox trend (similar slope).

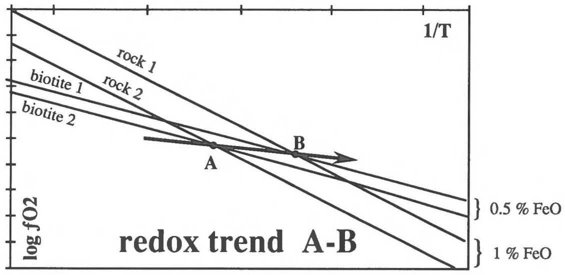

Fig. 3. Redox or cooling path defined by two samples, '1' and '2'. The graphical solution for T and log fO_2 results from the intersection of the lines 'rock 1' with 'biotite 1', and 'rock 2' with 'biotite 2'. The connection of the resulting two points, A and B, describes the redox trend. Geometry requires that those curves with the smallest separation, i.e. the biotite curves, determine the slope of the line A–B.

biotite crystallization are presented in the following. Graphically, these values are the intersection points of the two lines that represent the equations for rock and biotite. This graphic approach will be discussed below.

Results

Calculated temperatures and fO_2 values, as well as parameters used for the calculations for granites from Australia, Japan, N Portugal and the Alps are given in Tables 1a and b. LogfO_2 is plotted as a function of temperature (1/T) for these granites in Fig. 1. A summary plot of the fO_2-T regime for Australian and Japanese granites is shown in Fig. 2.

Results of T-fO_2 calculations are the following:

- Magnetite-granites plot at higher fO_2 values, i.e. between the NiNiO (NNO) and magnetite-hematite (MH) buffer, than ilmenite-granites.
- In T-fO_2 space, fields of magnetite- and ilmenite-granites are distinct and they describe an fO_2 range of 2, respectively 3 log units.
- A range of biotite crystallization temperatures up to 300° C may be encountered within a particular intrusion or suite.
- Most of the Australian and Portuguese ilmenite-granites plot below (FMQ).
- All Japanese ilmenite-granites and those from the Alps plot above (NNO).
- Magnetite- and ilmenite-granites from Japan and from the Alps are more oxidized than Australian and Portuguese granites.
- The T range for biotite crystallization in Australian granites is 200 degrees wider than for Japanese granites. Additionally, Australian granites crystallized on the average at higher temperatures.
- The redox trend is parallel to subparallel for all granites and oxidizing with respect to the buffers which means that the redox state of granites moves into the high-oxygen region of buffers during cooling.

Discussion

In order to interpret these results four principal questions have to be considered:

(1) why are all redox trends parallel to subparallel?
(2) what is the meaning of the temperature range for biotite crystallization?
(3) what is the reason for the different redox states and T ranges for granites from Australia and Japan?
(4) why is there no consistency between mineralogy and redox state for ilmenite-granites from Japan and those from the Alps?

Parallel to subparallel redox trend of granites

Figures 1 and 2 show that the redox trend is similar for all granites, i.e. a similarity in slope of the curves in the T-fO_2 diagrams. The reason for this similarity may be graphically elucidated, as done in Fig. 3

Here, for two granite samples, called '1' and '2', both equations, for biotite and bulk rock rock are plotted as logfO_2 verus 1/T. The intersections of biotite curves with those for the rock are marked as '*A*' and '*B*'. The line connecting '*A*' and '*B*' indicates the redox trend. The spatial separation between fO_2-1/T lines for biotite is usually smaller than for the rock, because variations in Fe^{2+}/Fe^{3+} of biotite are relatively small in comparison to those for the bulk rock. In Fig. 3, the distance between the lines corresponds to a difference of 0.5 wt.% FeO for biotite, and of 1 wt.% FeO for bulk rock. Geometric reasoning has it that those curves with the smallest separation determine the slope of the connecting line *A–B*, i.e. the biotite line. Figures 1 and 2 indicate that redox trends are similar, irrespective of the kind of granite. Such similarity in trend implies the same oxidizing redox trend for all granites upon cooling. An oxidizing trend has been assigned to open magmatic systems based on thermodynamical modelling (Ghiorso & Carmichael 1987). An oxidizing trend for all granites, on the other hand, is not in accordance with the statement of Wones & Eugster (1965) and Wones (1981) that magnetite-granites only follow an oxidizing trend in contrast to ilmenite-granites which follow a reducing trend.

Samples from the same intrusion, or the same magma system (most Australian granites), tend to plot on an approximately straight line, whereas plots of sets of samples representing suites or supersuites (Japanese granites) show inflections. The difference between a straight line for single intrusions versus inflected lines for suites and supersuites may be interpreted as being due to the difference between essentially one magma system, derived from one partial melting process, versus multiple systems, derived from different melting processes or different source rocks. Determination of T-fO_2 pairs thus offers a means of checking the cosanguinity of melts.

Rationalization of the T range

Magnetite and ilmenite occur in granites either as euhedral phenocrysts within feldspar or biotite, or interstitially in the groundmass. Whether Fe-Ti oxides crystallized before, during, or after biotite can therefore not be ascertained. Magnetite crystallization will withdraw a proportionally higher amount of Fe^{3+}, leaving the magma slightly more reduced, whereas ilmenite crystallization with its concomittant Fe^{2+} depletion would leave the magma slightly more oxidized. Crystallization of Fe-Ti oxides, because of their small percentage, was expected to have a minor effect on the redox state of the residual liquid of basic magmas (Carmichael 1991). The same may be assumed for granites which contain an even smaller amount of these opaques. The uncertainty regarding the relative timing of Fe-Ti oxide crystallization with respect to biotite is therefore irrelevant for the evolution of fO_2. Crystallization of several percent of biotite and amphibole leaves the remaining granite magma enriched in Fe^{3+} because of their low Fe^{3+}/Fe^{2+} ratio. Crystallization will occur stepwise because each batch of crystallized biotite (amphibole) leaves the residual too oxidized, i.e. with a too high Fe^{3+}/Fe^{2+} ratio for further biotite crystallization. Temperature and fO_2 have to decrease before a new batch of biotite is stable. This stepwise biotite crystallization may explain the spread of temperature and fO_2 values.

The calculation of T-fO_2 pairs traces the conditions of rock-biotite equilibrium at a certain temperature and fO_2, based on a determination of Fe^{2+}/Fe^{3+} in biotite and host rock. Besides the uncertainty regarding a preserved original equilibrium, the fact that the analyzed bulk rock contained biotite, may introduce another error. One may therefore expect that the analyzed Fe^{2+}/Fe^{3+} ratio of the rock (with its biotite) is too high. The increase in Fe^{2+}/Fe^{3+} ratio is opposite to that of postmagmatic alteration. The question to what extent we may assume cancellation of these two effects is discussed in the next section.

Table 1. Calculated temperatures, logfO_2 values and parameters used for the calculation for granites from (a) Australia and N Portugal (b) Japan and the Alps (Bergell). 'a' stands for the activity of sanidine (san) and magnetite (mt), respectively; Fe2+ is the number of ferrous iron ions in biotite (wet chemical analyses) per unit formula; and Fe# is the iron number of biotite, Fe/(Fe+Mg); lnXi/Xi stands for ln ($X_{Fe\ O(1.464)}$/$X_{Fe\ O}$), and ΣWi/Xi stands for the sum of the Margules terms. Descriptions of the granites, references, and some details on the calculations are given in the Appendix.

AUSTRALIA

	P[kbar]	a (san)	a (mt)	Fe2+ biotite	Fe# biotite	ln Xi/Xi bulk	Σ WiXi bulk	1/T *10 000	T [K]	log *f*O2
Jindabyne										
KB18	2.5	0.9	1	1.114	0.486	-0.84	-2.41	10.6	941	-14.7
KB5	2.5	0.9	1	1.058	0.434	-0.49	-2.56	11.2	893	-15.4
KB26	2.5	0.9	1	1.125	0.472	-0.83	-2.28	10.7	937	-14.8
KB29	2.5	0.9	1	1.090	0.462	-0.65	-2.75	10.9	920	-15.0
KB34	2.5	0.9	1	1:263	0.568	-1.19	-2.17	10.0	996	-14.0
Strathbogie										
Str 129	4.0	0.9	0.2	1.572	0.669	-3.32	-2.87	7.7	1299	-13.0
Str 126	4.0	0.9	0.2	1.319	0.654	-2.74	-2.62	8.2	1225	-12.9
Str 122	4.0	0.9	0.2	1.606	0.680	-3.09	-2.53	8.2	1215	-13.7
Str 142	4.0	0.9	0.2	1.541	0.671	-2.95	-2.67	8.5	1178	-14.0
Str 135	4.0	0.9	0.2	1.562	0.635	-2.77	-2.78	8.8	1134	-14.4
Str 120	4.0	0.9	0.2	1.538	0.667	-3.16	-2.80	8.0	1243	-13.4
Stawell										
WV196	2.5	0.9	1	1.417	0.553	-0.95	-3.66	10.7	930	-15.5
WV197	2.5	0.9	1	1.344	0.567	-1.13	-3.64	10.3	968	-14.9
WV198	2.5	0.9	1	1.373	0.573	-1.93	-3.53	9.0	1115	-13.3
Tynong										
CV 103	1.0	0.9	0.2	1.450	0.578	-3.09	-3.45	9.1	1097	-15.8
CV 104	1.0	0.9	0.2	1.360	0.535	-3.37	-3.32	8.5	1176	-14.9
CV 67	1.0	0.9	0.2	1.584	0.632	-1.54	-3.71	11.8	845	-19.1
CV 65	1.0	0.9	0.2	1.794	0.712	-1.72	-3.94	11.8	850	-19.3
CV 86Ly	1.0	0.9	0.2	1.321	0.528	-2.07	-1.55	11.0	906	-17.7
Cabanandra										
BG7	2.0	0.9	1	1.349	0.560	-1.08	-2.56	10.8	928	-15.5
BG38	2.0	0.9	1	1.419	0.556	-1.31	-2.49	10.5	951	-15.4
BG37	2.0	0.9	1	1.242	0.538	-1.14	-2.56	10.5	956	-15.0
BG32	2.0	0.9	1	1.281	0.529	-1.34	-2.68	10.2	985	-14.7

N PORTUGAL

	P[kbar]	a (san)	a (mt)	Fe2+ biotite	Fe# biotite	ln Xi/Xi bulk	Σ WiXi bulk	1/T *10 000	T [K]	log *f*O2
'1'	2.5	0.9	0.2	0.955	0.477	-1.76	-4.13	9.6	1044	-14.5
'8'	2.5	0.9	0.2	1.100	0.511	-2.90	-3.99	7.8	1274	-12.7
'9'	2.5	0.9	0.2	1.134	0.478	-1.95	-3.93	9.7	1029	-15.1
'11'	2.5	0.9	0.2	1.206	0.543	-2.88	-3.53	8.2	1214	-13.5
'12'	2.5	0.9	0.2	1.306	0.586	-2.55	-3.21	9.1	1095	-14.8
'13'	2.5	0.9	0.2	1.239	0.596	-2.67	-3.37	8.7	1144	-14.2
'14'	2.5	0.9	0.2	1.331	0.600	-2.69	-3.48	8.9	1127	-14.5
'16'	2.5	0.9	0.2	1.375	0.658	-2.37	-3.80	9.5	1055	-15.3

Data based on De Albuquerque (1971, 1973)

JAPAN

	P[kbar]	a (san)	a (mt)	Fe2+ biotite	Fe# biotite	ln Xi/Xi bulk	Σ WiXi bulk	1/T *10 000	T [K]	log *f*O2
CHUGOKU										
Daito										
6412-17	1	0.8	1	0.935	0.435	-0.54	-2.34	11.4	877	-15.9
6510-116	1	0.8	1	0.906	0.410	-0.09	-3.13	11.9	841	-16.3
6510-132	1	0.8	1	0.803	0.379	0.55	-3.19	12.6	792	-16.8
Hiroshima										
H-72	1	0.95	0.2	1.260	0.560	-1.53	-2.93	11.4	875	-17.9
H-89	1	0.95	0.2	1.154	0.495	-1.00	-3.25	12.0	833	-18.3
H-93	3	0.8	0.2	1.574	0.682	-1.09	-3.70	12.0	835	-18.5
Takanawa										
MY-15	3.5	0.95	0.2	1.166	0.513	-1.39	-2.85	10.7	938	-15.9
MY-6	3.5	0.95	0.2	1.432	0.320	-1.08	-3.15	11.6	861	-17.6
MY-2	3.5	0.95	0.2	1.682	0.720	-0.99	-3.56	12.0	830	-18.5
MY-1	3.5	0.95	0.2	1.804	0.772	-0.28	-4.03	13.2	755	-19.9
CHUBU										
Hatogaya										
RS-88	5	0.85	1	1.325	0.560	-0.85	-4.14	9.9	1008	-13.6
RS-87	5	0.85	1	1.208	0.546	0.15	-3.61	11.5	868	-15.2
RS-91	5	0.85	1	1.230	0.556	1.22	-3.96	13.2	755	-17.1
Toki										
T-41	3	0.9	0.2	1.439	0.658	-1.63	-2.55	11.3	887	-17.7
T-38	3	0.85	0.2	1.527	0.660	-1.85	-3.33	10.6	940	-16.9
T-44	3	0.9	0.2	1.810	0.885	-0.99	-3.51	12.4	805	-19.3
T-25	3	0.9	0.2	1.804	0.875	-1.87	-3.73	10.9	918	-17.6
Ryoke I										
T-97	3	0.9	0.2	1.449	0.635	-1.78	-2.99	10.7	937	-16.7
T-94	4.5	0.8	0.2	1.595	0.730	-1.10	-3.34	11.6	861	-17.6
T-145	4.5	0.9	0.2	1.640	0.736	-1.42	-3.10	11.1	901	-17.0
Ryoke II										
T-75	5	0.9	0.2	1.473	0.676	-1.61	-2.16	10.6	948	-15.9
T-165	4.5	0.95	0.2	1.479	0.638	-1.54	-3.50	10.5	952	-16.0
T-168	4.5	0.95	0.2	1.410	0.639	-1.63	-2.93	10.4	966	-15.7
Ryoke III										
T-76	4.5	0.9	0.2	1.433	0.683	-1.77	-2.19	10.4	965	-15.8
T-133	4.5	0.9	0.2	1.413	0.701	-1.38	-3.41	10.7	932	-16.2

Data based on Ishihara & Terashima (1977) and Czamanske et al. (1981)

ALPS (BERGELL)

	P[kbar]	a (san)	a (mt)	Fe2+ biotite	Fe# biotite	ln Xi/Xi bulk	Σ WiXi bulk	1/T *10 000	T [K]	log *f*O2
Berg 3a	3.5	0.9	1	1.045	0.509	-0.74	-4.16	10.0	1000	-13.5
Berg 21	3.5	0.9	1	1.004	0.491	-1.07	-3.67	9.4	1063	-12.7
Berg 191	3.5	0.9	1	0.940	0.448	-0.92	-3.89	9.5	1057	-12.6
Berg 11b	3.5	0.9	1	0.970	0.472	-1.09	-4.08	9.2	1088	-12.4
Berg 18a	3.5	0.9	1	1.048	0.493	-1.40	-4.09	8.8	1133	-12.1
Berg 7	5.0	0.9	0.2	0.943	0.436	-1.34	-3.95	9.6	1045	-13.6
Berg 6	5.0	0.9	0.2	0.934	0.436	-1.84	-4.10	8.6	1168	-12.3

Data from Burkhard (unpubl.)

Redox state of granites – the subtle role of H_2O

The large range of redox states known from granites suggests a variety of possible controlling parameters for fO_2 and corresponding interpretations:

Previous discussions on the origin of fO_2

It has been frequently assumed that the thermal dissociation of water and subsequent loss of hydrogen, controls the oxidation state of a magma (e.g. Eugster & Wones 1962, Wones & Eugster 1965, Czamanske & Wones 1973, Czamanske et al. 1981). In Japan, an alternative school claims that organic carbon is responsible for the reduced redox state of granites derived from sediments. It has also been suggested that the redox state of a magmatic rock reflects its source (Wones 1989, Carmichael 1991).

The variety of redox states of granites and a comparison to volcanic rocks

The variety of granites with different types of redox states includes granites such as the Australian ones which are quite reduced. For these, one may argue that their redox state reflects the redox state of their source rock. A second group comprises granites like the magnetite-granites from the Finnmarka Complex in the Oslo Graben, for which Czamanske & Wones (1973) demonstrated that oxidation occurred during biotite crystallization. In a third group fall ilmenite-granites like those from Japan. They are magnetite-free, suggesting a redox state below (FMQ) but their redox state is calculated to be above (FMQ) (Fig. 1). Similar observations were made by Dillet & Czamanske (1987) on some ilmenite-granites from the Questa Caldera, New Mexico, and by myself (unpubl.) from Bergell intrusives in the Alps. These ilmenite-granites commonly contain titanite, either primary, or secondary as a replacement of ilmenite.

Apparently, this discrepancy between the calculated redox state and that inferred from the mineralogy is restricted to plutonic rocks. In Tertiary to Recent volcanic rocks, Ewart (1979) assigned distinct and characteristic redox states to volcanic rocks of a particular region, leading to the conclusion that fO_2 is intrinsic to the rock and specific to a region. Similarly, Carmichael (1991) suggested that the redox state of basic and silicic volcanic magmas reflects the redox state of the source.[2]

If this variety of redox states of granitic rocks is to be explained, a common mechanism as to its origin has to be found that suits all cases. Because granitic magmas contain a substantially higher amount of water than their extrusive equivalents, it is the water that may be expected to be important for such a mechanism. In the following a mechanism is suggested that considers the role of water in relation to the redox state of granites.

H_2O: the controlling parameter for fO_2; the mechanism

The solubility of H_2O in a melt increases with temperature and pressure.[3] Upon cooling the water solubility decreases and its saturation point is reached at a temperature that is related to the amount of water dissolved in the magma and that is inversely related to pressure. Only below this temperature, i.e. during subsequent cooling, may H_2O oxidize the magma or crystallizing phases, as discussed below. This means that at a given pressure the amount of water dissolved in a magma prior to cooling will determine the water saturation temperature and thus

---

[2] Based on stable isotope date by Hildreth et al. (1984) Carmichael argues that an intensive interaction of meteoric water with the magma did not affect the redox state of Fe-Ti oxides. This argumentation is not too obvious, because firstly, Hildreth et al. (1984) themselves express doubts on the interaction with ^{18}O-depleted meteoric water; secondly, isotope exchange processes are much debated because of a lack of sufficient experimental data on this process (some problems and inconsistencies related to assumptions of isotope exchange have been pointed out by Burkhard & O'Neil 1988); thirdly, the availability of water to such an extent as to exchange ^{18}O would undoubtedly result in some kind of Fe oxidation.

[3] Reactions between the silica and H_2O. Molecular orbital calculation performed by De Jong and Brown (1980b) showed how H_2O is absorbed by silica liquids; by exothermic reactions, H^+, H_3O^+ and H_2O are attached to bridging oxygen O_{br} (O_{br} has a high electron donor capacity, De Jong and Brown 1980a; Burkhard et al. 1991), and H^- and OH^+ are attached to O_{nbr}. Therefore, De Jong & Brown concluded that the solubility of H_2O in melts depends on the ease with which Si-O_{br} bonds can be broken. This depolymerization effect is in agreement with the experimentally determined decrease of viscosity in the presence of water (Eggler & Rosenhauer 1978). It is obvious that the Si-O_{br} bonds can be broken more easily at higher temperatures, a fact which explains why the solubility of water increases with temperature.

the upper temperature for magma and mineral oxidation; the temperature of magma oxidation can be expected to equal at best the water saturation temperature T_{H2O} but is probably lower.

Qualitatively, three cases may be distinguished:
(1) $T_{H2O} \geqslant T_{bio\ cryst}$
(2) $T_{H2O} < T_{bio\ cryst}$
(3) $T_{H2O} << T_{bio\ cryst}$

(1) $T_{H2O} \geq T_{bio\ cryst}$

For a magma containing a high amount of water, water saturation temperature may be approximately that for biotite crystallization. Hence, crystallizing biotite is oxidized causing crystallization of magnetite. Figure 4a illustrates the oxidation of such a granite; the intersection is shifted towards higher fO_2 values (less negative log fO_2 compared to 'rock 1') and lower temperatures. Granites formed under these conditions will always be magnetite-granites.

(2) $T_{H2O} < T_{bio\ cryst}$

For a magma containing a lower amount of water, water saturation temperatures are below that of biotite crystallization and oxidation by water will not affect biotite, but later crystallizing mineral phases, i.e. 'the rock'. This case is illustrated in Fig. 4b.

Such a granite will be either a magnetite-granite, or an ilmenite-granite which was originally below (FMQ) but became oxidized during crystallization such that it plots now above (FMQ).

(3) $T_{H2O} << T_{bio\ cryst}$

For a magma containing a very small amount of water, water saturation temperature will occur when all mineral phases have been crystallized. Oxidation by water will, if at all, occur as a postmagmatic, hydrothermal alteration. Granites formed under these conditions are likely to preserve the redox state of their source rock.

The above temperature relationships depend on $T_{bio\ cryst}$ which may vary by several hundred degrees, and they depend on the ambient pressure because of the pressure dependence of T_{H2O}. The lower temperature limit for T_{ox} ($\leq T_{H2Osat}$) may be 500± 50° C, the temperature where Fe-Ti oxides re-equilibrate due to hydrothermal or postmagmatic water in granites.

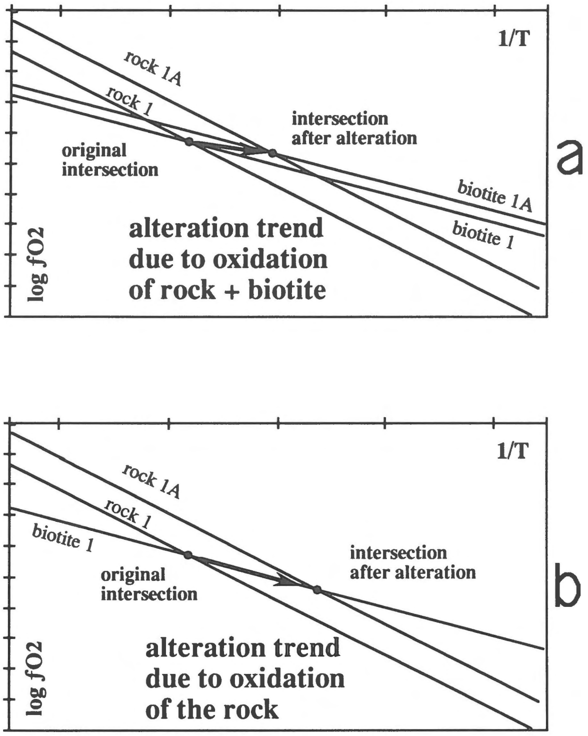

Fig. 4. Graphical illustration of any late oxidation on the T-logfO_2 values for a sample '1'; '1A' stands for altered, i.e. oxidized. (a) alteration caused by an oxidation-alteration that affects the rock and biotite. This is the case if $T_{H2O} \geq T_{bio\ cryst}$. (b) alteration caused by an oxidation-alteration that affects the rock only. This is the case for $T_{H2O} > T_{bio\ cryst}$ (see text).

The original amount of water dissolved prior to cooling cannot be estimated because of devolatilization of a magma upon cooling. Therefore, a cross check of my concept is not possible by means of theoretical or experimental results on water solubility.

Relation to granite emplacement

A distinction between these three conditions of granite formation which depend on the water availability during emplacement, can be inferred from the redox state of ilmenite-granites. Ilmenite-granites which are below (FMQ) have experienced no or little oxidation. They fall in the third category and their redox state reflects that of their source rock. Ilmenite-granites above (FMQ) have experienced oxidation and they fall in the second category. Ilmenite-granites cannot be found under conditions of the first category because oxidation around temperatures of biotite crystallization results in magnetite information, according to the equation: biotite + O_2= magnetite + sanidine + H_2O. Ilmenite-granites therefore serve as indicator of the redox environment of granite emplacement.

The T-fO_2 data of granites presented here show that ilmenite-granites plot consistently either below or above (FMQ) for a particular region (Fig. 1). This regional dependence suggests that the preservation of a redox state, or oxidation during crystallization, as observed for some ilmenite-granites, holds for magnetite-granites as well. The idea finds support in the overall similar characteristics of both, magnetite- and ilmenite-granites of a particular region. Granites of this study are categorized according to T_{H2O} versus T_{bio} as indicated in Table 2.

The regional dependence of redox states suggests that the driving force itself, the water content of these magmas, may be a regional characteristic. This touches upon a possible relation to the tectonic setting for at least the Australian and Japanese granites which cover larger regions. The tectonic setting for Japanese granites is in an extensional regime of a continent-ocean collision environment which itself is subduction-related. A similar tectonic setting is known from the Questa Caldera, New Mexico, for which oxidation during crystallization has been discussed by Dillet & Czamanske (1987). Granites from N Portugal, on the other hand, are known not to be subduction-related. Although the tectonic setting of Australian granites is not yet clear, it is likely that they are also not related to subduction (Chappell 1984). Such relations between granite types and tectonic environment have been already suggested by Pitcher (1982), based on chemical variations. A relationship between tectonic settings and redox state coupled with temperature during crystallization opens up an avenue to relate the tectonic environment to different mechanisms of granite magma genesis and emplacement in addition to chemical variability. A principal question that needs answering concerns the source of water. This is subject of ongoing research.

Conclusions

A comparison of granites based on T-fO_2 estimation (Burkhard 1991) shows that:

(1) The redox state may be intrinsic to a rock, i.e. a reflection of the source rock. However, the original redox state may also be overprinted to

Table 2. Summary of the three possible relations between temperature of biotite crystallization T_{bio} and oxidation of the rock, the onset of which is below the temperature of water saturation of the magma T_{H2O}. The third column contains the regional examples discussed in the text.

	mt-granites	**ilm-granites**	**Region**
$T_{H2O} << T_{bio}$	reflects the source	reflects the source	Australia, Portugal
$T_{H2O} < T_{bio}$	oxidized rock (Fig.4b) related ilm-granites plot above FMQ	oxidized rock (Fig.4b) plot above FMQ	Japan, Alps (Bergell) New Mexico (Questa Caldera)
$T_{H2O} \geq T_{bio}$	biotite is oxidized mt formation	(not possible)	Oslo Graben

T_{H2O}: water saturation temperature of the magma

T_{bio}: crystallization temperature of biotite various degrees by oxidation during crystallization. Granites which preserved the redox state of their source rock occur in Australia and N Portugal; in contrast, Japanese granites have been oxidized during crystallization. This distinction is possible on the basis of the redox state of ilmenite-granites. They plot below (FMQ) if granites preserved their original redox state, and above (FMQ) if oxidation occurred.

(2) The redox states of granites prove to be consistent for regions with a specific tectonic setting; granites that were oxidized during crystallization occur in a subduction-related environment whereas granites with a redox state inherited from their source rock occur in a non-subduction-related environment.

(3) The degree of oxidation of a magma depends on the amount of water dissolved in the magma prior to cooling. This water content determines the water saturation temperature. Below this saturation temperature the magma may become oxidized due to interaction with water.

(4) The amount of water available during granite emplacement may largely depend on the tectonic setting.

These results open up a perspective for a causal relationship between water content and source on the one hand, and mechanisms and conditions of granite genesis and emplacement on the other.

Acknowledgements

I thank Allan J.R. White and B.C. Chappell who generously made available samples from Australian granites as well as their bulk rock analyses. Shunso Ishihara provided information and advice for a suitable selection of data on Japanese granites. I carried out the analytical work at the Department of Geology at the University of Melbourne with a research fellowship of the 'Deutsche Forschungsgemeinschaft' in the years 1988–1990. This support is very much appreciated. Constructive criticism by Bernard H.W.S. de Jong considerably improved the manuscript.

Appendix

Description of the granites

Five granites from the Lachlan Fold Belt, Australia, selected for this study, include I-type, magnetite-, S-type, ilmenite-, I-type, ilmenite-, and S-type, magnetite-granites. They are listed below with further references.

I-type, magnetite-granite: Jindabyne, 412.7± 9 Ma (Jindabyne Suite, Kosciusko Batholith) tonalite with hornblende, biotite (simultaneous crystallization), apatite, titanite, abundant magnetite, some ilmenite. P = 2.5 kb (hornblende geobarometer). *White et al. (1977), Hine et al. (1978), Burkhard (1991)*

S-type, ilmenite-granite: Strathbogie, 365 ± 6 Ma granite with garnet, cordierite, biotite, ilmenite, pyrrhotite. P = 4 kb *Hine et al. (1978), Phillips et al. (1981), Clemens & Wall (1981), Richards & Singleton (1981), White (1988), White & Chappell (1988), Burkhard (1991).*

I-type, ilmenite-granite: Tynong and Lysterfield, 371 ± 12 Ma (Tynong Suite) granodiorite with small amounts of hornblende intergrown with biotite, ilmenite, allanite, prim. garnet, apatite, pyrrhotite, chalcopyrite, covelline. P = 1 kb (hornblende geobarometer). *Richards & Singleton (1981), White (1988), White & Chappell (1988)*

I-type, magnetite-granite: Stawell, 396 ± 5 Ma (Ararat Suite) granodiorite with hornblende, magnetite, ilmenite, allanite, chalcopyrite. P = 2.5 kb (hornblende geobarometer). *White (1986), White (1988), White & Chappell (1988)*

S-type, magnetite-granite: Cabanandra, ca. 420 Ma (Dalgety Suite, Bonang Batholith) granites with biotite, cordierite, hypersthene, magnetite with ilmenite exsolution, apatite, zircon, monazite. P = 2 kb (A.J.R. White, pers. comm) *White (1988), White & Chapell (1988)*

Electron microprobe analyses were carried out with a Cameca SX 50, operating at 15 keV and 25 nA. Natural standards used for the silicates were: wollastonite (Si and Ca), periclase (Mg), hematite (Fe), rutile (Ti), jadeite (Na), benitoite (Ba), K-tantalite (K), NaCl (Cl), apatite (P). Synthetic standards include: Al_2O_3 (Al), NaF_4 (F), and pure Cr and Zn for Cr and Zn respectively. Oxides were analyzed with the same standards used for the silicates and in addition pure Mn and V for these elements, respectively. A description of the wet chemical analyses of ferrous iron is described in Burkhard (1991). Data on the bulk chemistry have been made available by A.J.R. White & B.W. Chappell.

The Australian granites are characterized by three Harker diagrams showing the SiO_2, Fe, and Fe/Mg distribution of the bulk rock (Fig. 5), and the biotite chemistry Al^{IV} vs $Fe_{tot}/(Fe_{tot} + Mg)$ (Fig. 6).

The Fe and Mg chemistry of biotite is not directly or inversely related to the bulk rock chemistry of granites as a comparison of Figs 5 and 6 indicates. Instead, Fe partitioning is controlled by the oxygen fugacity such that biotite crystallization at a low fO_2 will partition Fe, mainly as Fe^{2+}, into biotite and ilmenite (ilmenite-granite), and, at high fO_2, Fe will be used to crystallize magnetite, whereas biotite will become Mg-rich (magnetite-granite),

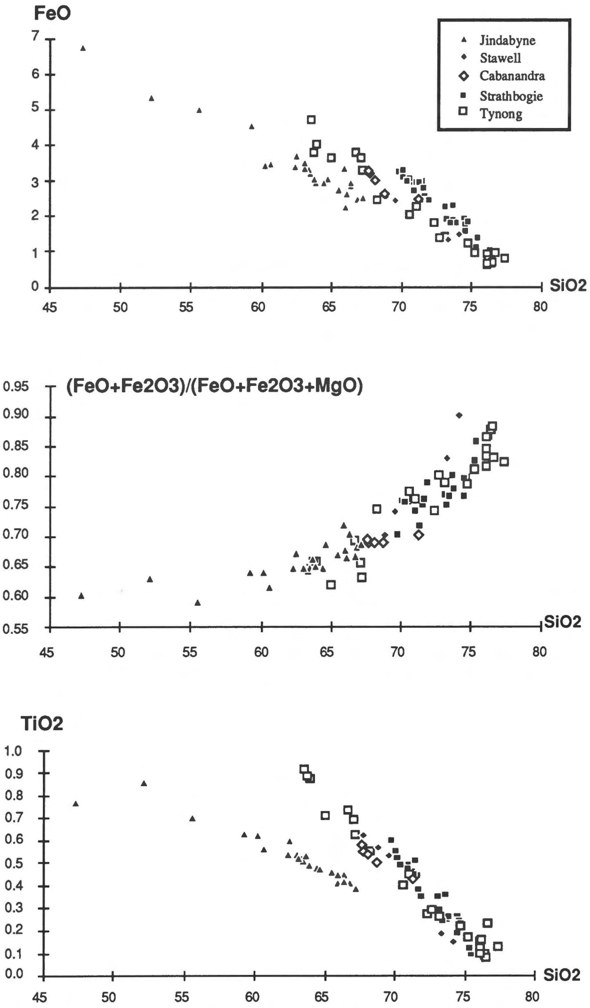

Fig. 5. Harker diagrams of FeO, FeO(tot)/FeO(tot)+ MgO, and TiO_2 vs SiO_2 for Australian granites of the Lachlan Fold Belt.

as stated by Wones & Eugster (1965), Czamanske & Wones (1973) and Ishihara (1977, 1981).

The crystallization temperature of biotite is estimated from:

$$T = \frac{1}{4c_2}\{-k_1 - 2c_1 \pm \sqrt{[(k_1 + 2c_1)^2 + 8c_2k_2]}\} \qquad \text{Burkhard (1991)}$$

with:

k_1: $-23.74 - 6\log X_{Fe^{2+}} + 2\log a_{san} + 2\log a_{mt} - \ln (X_{FeO\ (1.464)}/X_{FeO})$

k_2: $-11951.68 + 225.06\ \Sigma\Delta W_iX_i - 0.022(P\text{-}1000)$

where T is temperature in degrees K, P is pressure in bar, $X_{Fe^{2+}}$ is the number of ferrous ions in biotite, divided by three (number of octahedral sites per unit formula), 'a' is the activity for magnetite (mt) and K-feldspar (san), ΔW_iX_i are the Margules terms, for Al_2O_3: 49.04; CaO: −48.87; Na_2O: −106.04; K_2O: −110.46 in kJ,

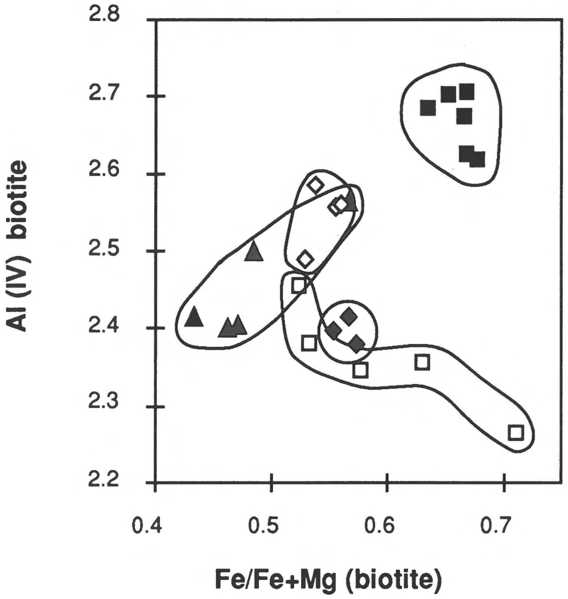

Fig. 6. Al^{IV} vs Fe/(Fe+Mg) chemistry of biotite occurring in granites of the Lachlan Fold Belt. Symbols mean the same as those used in Fig. 5. A comparison with Fig. 5 shows that there is no relation between the Fe content of the rock and the Fe content of the biotite.

respectively, X_i is the mole fraction of the subscripted species i in the melt (Kress & Carmichael (1988).
c_1 and c_2 are the two coefficients of the linear approximation for log fH_2O, which may be estimated from total pressure during crystallization from Burnham et al. (1969). For details see Burkhard (1991).

The corresponding fO_2 may be back-calculated from Kress & Carmichael (1988):

$$0.232 \ln fO_2 = \frac{\Delta H + \Sigma\Delta W_iX_i}{RT} - \frac{\Delta S}{R} + \ln \frac{X_{FeO}\,(1.464)}{X_{FeO}}$$

where ΔW_iX_i and X_i are defined as above, and ΔH and ΔS are the enthalpy and the entropy for the reaction: 2FeO(melt)+ $0.5O_2$(gas) = Fe_2O_3(melt) (−95.93 kJ and −46.06 J/K, respectively), R is the gas constant, and T is the crystallization temperature of biotite, as calculated above.

References

Buddington, A.F. & D.H. Lindsley 1964 Iron-titanium oxide minerals and synthetic equivalents – J. Petrol. 5: 310–420

Burkhard, D.J.M. 1991 Temperature and redox trend of biotite-bearing rocks: a method of estimation applied to S- and I-type granites from Australia-Earth Planet. Sci. Lett. 104: 89–98

Burkhard, D.J.M. & J.R. O'Neil 1988 Contrasting serpentinization processes in the eastern Central Alps – Contrib. Mineral. Petrol. 99: 498–506

Burkhard, D.J.M., B.H.W.S. de Jong, A.J.H.M. Meyer & J.H. van Lenthe 1991 $H_6Si_2O_7$: *Ab Initio* molecular orbital calculations show two geometric conformations – Geoch. Cosmochimica Acta, Lett. 55: 3453–3458

Burnham, C.W., J.R. Holloway & N.F. Davis 1969 Thermodynamic properties of water to 1000° C and 10 000 bars – Geol. Soc. Am. Spec. Pap. 132, 96p

Carmichael, I.S.E. 1991 The redox state of basic and silicic magmas: a reflection of their source regions? – Contrib. Mineral. Petrol. 106: 129–141

Chappell, B.W. 1984 Source rocks of I- and S-type granites in the Lachlan Fold Belt, southeastern Australia – Phil. Trans. R. Soc. London A 310: 693–707

Clemens, J.D. & V.J. Wall 1981 Origin and crystallization of some peraluminous S-type granitic magmas. Canad. Mineral. 19: 111–131

Czamanske, G.K., S. Ishihara & S.A. Atkin 1981 Chemistry of rock-forming minerals of the Cretaceous-Paleocene batholith in southwestern Japan and implications for magma genesis – J. Geophys. Res. 86: 10431–10469

Czamanske, G.K. & D.R. Wones 1973 Oxidation during magmatic differentiation, Finnmarka Complex, Oslo Area, Norway: part 2, The mafic silicates – J. Petrol. 14: 349–380

De Albuquerque, C.A.R. 1971 Petrochemistry of a series of granitic rocks from northern Portugal – Geol. Soc. Am. Bull. 82: 2783–2798

De Albuquerque, C.A.R. 1973 Geochemistry of biotites from granite rocks, Northern Portugal – Geoch. Cosmochimica. Acta 37: 1779–1802

De Jong, B.H.W.S. & G.E. Brown Jr 1980a Polymerization of silicate and aluminate tetrahedra in glasses, melts, and aqueous solutions – I. Electronic structure of $H_6Si_2O_7$, $H_6AlSiO_7{}^{1-}$, and $H_6Al_2O_7^{2-}$. – Geoch. Cosmochimica Acta 44: 491–511

de Jong, B.H.W.S. & G.E. Brown Jr 1980b Polymerization of silicate and aluminate tetrahedra in glasses, melts, and aqueous solutions – II. The network modifying effects of Mg^{2+}, K^+, Na^+, Li^+, H^+, OH^-, F^-, Cl^-, H_2O, CO_2 and H_3O^+ on silicate polymers – Geoch. Cosmochimica Acta 44: 1627–1642

Dillet, B. & G.C. Czamanske 1987 Aspects of petrology, mineralogy, and geochemistry of the granitic rocks associated with Questa Caldera, Northern New Mexico. U.S. Geological Survey, Open-File Report 87–258: p. 238

Eggler, D.H. & M. Rosenhauer 1978 Carbon dioxide in silicate melts. 2. Solubilities of CO_2 and H_2O in $CaMgSi_2O_6$ diopside liquids and vapors at pressures to 40 Kb – J. Geology 278: 64–94

Eugster, H.P. & D.R. Wones 1962 Stability relations of the ferruginous biotite, annite – J. Petrol. 3: 82–125

Ewart, A. 1979 A review of the mineralogy and chemistry of Tertiary-Recent dacitic, latitic, rhyolitic and related salic volcanic rocks. In: F. Barker (ed.) Trondhjemites, dacites and related rocks, Springer, Berlin: 12–101

Ghiorso, M.S. & I.S.E. Carmichael 1987 In: I.S.E. Carmichael & H.P. Eugster (eds.) Modelling magmatic systems: petrologic applications. Rev. Mineral. 17: 467–499

Hildreth, W., R.L. Christiansen & J.R. O'Neil 1984 Catastrophic isotopic modification of rhyolitic magma at times of caldera subsidence, Yellowstone Plateau volcanic field. J. Geophys. Res. 89: 8339–8369

Hine, R., I.S. Williams, B.W. Chappell & A.J.R. White 1978 Contrasts between I-and S-type granitoids of the Kosciusko Batholith – J. Geol. Soc. Australia 25: 219–234

Hollister, L.S., G.C. Grissom, E.K. Peters, H.H. Stowell & V.B. Gisson 1987 Confirmation of the empirical correlation of Al in hornblende with pressure of solidification of calc-alkaline plutons. Am. Mineral. 72: 231–239

Huebner, J.S. 1971 Buffering Techniques for Hydrostatic Systems at Elevated Pressures, 123–177. In: G.C. Ulmer (ed.) Research techniques for high pressures and high temperatures, Springer, Berlin.

Ishihara, S. 1977 The magnetite-series and ilmenite-series granitic rocks – Mining Geology 27: 293–305

Ishihara S. 1981 The granitoid series and mineralization – Econ. Geol. 75th Ann. Issue: 458–484

Ishihara S. & S. Terashima 1977 Chemical variation of the Cretaceous granitoids across southwestern Japan – Shirakawa-Toki-Okazaki-transection – J. Geol. Soc. Japan 83: 1–18

Kress, V.C. & I.S.E. Carmichael 1988 Stoichiometry of the iron oxidation reaction in silicate melts – Am. Mineral. 73: 1267–1274

Phillips, G.N., V.J. Wall & J.D. Clemens 1981 Petrology of the Strathbogie Batholith: A Cordierite-Bearing Granite – Canad. Mineral. 19: 47–63

Pitcher, W.S. 1982 Granite type and tectonic environment. In: K.J. Hsü (ed.) Mountain building processes, Academic Press, London.

Richards, J.R. & O.P. Singleton 1981 Palaezoic Victoria, Australia: igneous rocks, ages and their interpretation – J. Geol. Soc. Australia 28: 395–421

White, A.J.R. 1986 Granites around Ballarat Ararat and Stawell. Amira Field Excursion, La Troube Univ., Melbourne, December 1986: 12p

White, A.J.R. 1988 Intrusive rocks of Victoria: In:: I. Clark & B. Cook (eds.) Victorian Geology, Excursion Guide, Australian Academy of Science: 57–66

White, A.J.R. & B.W. Chappell 1988 Granites, petrology and igneous rocks: In: J.G. Douglas & J.A. Ferguson (eds.) Geology of Victoria – Victorian Div. Geol. Society of Australia: 427–439

White, A.J.R., I.S. Williams & B.W. Chappell 1977 Geology of the Berridale 1:100 000 sheet 8625 – Geol. Survey New South Wales, Dept. Mines: 138 p

Wones, D.R. 1963 Physical properties of synthetic biotites on the join phlogopite-annite – Am. Mineral. 48: 1300–1322

Wones, D.R. 1981 Mafic silicates as indicators of intrusive variables in granitic magmas – Mining Geology 31: 191–212

Wones, D.R. 1989 Significance of the assemblage titanite + magnetite + quartz in granitic rocks – Am. Mineral. 74: 744–749

Wones, D.R. & H.P. Eugster 1965 Stability of biotite: experiment, theory, and application – Am. Mineral. 50: 1228–1272